Dalton Transactions

PAPER

View Article Online
View Journal | View Issue

Cite this: *Dalton Trans.*, 2018, **47**, 6549

An investigation of the roles furan *versus* thiophene π-bridges play in donor–π-acceptor porphyrin based DSSCs†

Michele Cariello, ‡[a] Saifaldeen M. Abdalhadi,‡[a] Pankaj Yadav,[b] Jean-David Decoppet,[b] Shaik M. Zakeeruddin, *[b] Michael Grätzel,[b] Anders Hagfeldt [c] and Graeme Cooke *[a]

Dye-sensitized solar cells (DSSCs) continue to attract interest due to their lower cost production compared to silicon based solar cells and their improving power conversion efficiencies. Porphyrin-based sensitizers have become an important sub-class due to their strong absorption characteristics in the visible region, convenient modulation of properties through synthetic manipulation and class-leading power conversion efficiencies. In this article, we report the synthesis and characterization of two porphyrin-based dyes and their application as sensitizers in DSSCs. A thiophene and a furan moiety have been incorporated into the push–pull architecture as a π-bridge, allowing the systematic investigation of how these moieties influence the physical properties of the dyes and the performance of their resulting DSSCs. A significant difference in PCEs has been observed, with the furan containing dye (**PorF**, PCE = 4.5%) being more efficient than the thiophene-based analogue (**PorT**, PCE = 3.6%) in conjunction with the iodide/triiodide redox electrolyte.

Received 31st January 2018,
Accepted 19th April 2018

DOI: 10.1039/c8dt00413g

rsc.li/dalton

Introduction

Photovoltaics (PV) offer an attractive renewable energy technology and there is a continued interest in this field due to the potentially inexhaustible energy source provided by sun.[1] During the last twenty years, interest in dye-sensitised solar cells (DSSCs) as promising PV technology has increased, due to their ease of fabrication, relatively low cost and interesting design possibilities in terms of tunable transparency and colour. Since the development of the first working device in 1991 by Grätzel and O'Reagan,[2] there has been a huge effort directed towards increasing the power conversion efficiency (PCE) of devices by optimising their components, with a particular emphasis being placed on the sensitiser, as it determines the light harvesting and absorption properties of the device. Ruthenium-based dyes, such as N719, have monopolised the early progress in this field, however, metal-free organic dyes have become increasingly attractive due to their lower cost, together with higher molar extinction coefficients, easier synthesis, purification and structural modification.[3]

More recently, the development of porphyrin-based dyes has revitalised research in metal-incorporating dyes, due to the employment of less expensive metals (such as Zn, instead of Ru), their synthetically tunable optical properties and good photostability.[4–6] In particular, the position of these bands, together with the redox properties,[7,8] can be tuned through the insertion of a metal in the central cavity[9] and through the substitution of the porphyrin periphery, which can be done by functionalising the β-positions and the *meso*-positions. While zinc is the most preferred metal due to its low-cost and ability to broaden the optical absorption of porphyrins,[10] the types of substituent that could be added to the peripheral positions to tune the properties of porphyrin derivatives is enormous.

Since the first report of a porphyrin-based sensitiser providing a PCE of 2.6%,[11] significant effort has been directed towards understanding the role substituents play on modulating the device characteristics of porphyrin based DSSCs. Functionality attached to both β- and *meso*-positions have been investigated, with the latter typically providing the best performing dyes.[12] However, the performance of this class of dyes is generally lower than that of the most efficient Ru-based

[a]*WestCHEM, School of Chemistry, University of Glasgow, Glasgow, G12 8QQ, UK. E-mail: graeme.cooke@glasgow.ac.uk*
[b]*Laboratory of Photonics and Interfaces, Institute of Chemical Sciences and Engineering, École Polytechnique Fédérale de Lausanne, 1015 Lausanne, Switzerland. E-mail: shaik.zakeer@epfl.ch*
[c]*Laboratory of Photomolecular Science, Institute of Chemical Sciences and Engineering, École Polytechnique Fédérale de Lausanne, 1015 Lausanne, Switzerland*
†Electronic supplementary information (ESI) available. See DOI: 10.1039/c8dt00413g
‡These authors contributed equally.

dyes, due to their poor injection yields.[13,14] To circumvent this issue, the development of *meso*-substituted porphyrin dyes featuring a D–π-A architecture represents a step forward regarding the performance of these molecules in DSSCs.[15,16] In particular, substituting the porphyrin core with electron donating moieties and electron withdrawing units attached at opposite sides of the porphyrin ring, results in the generation of an intrinsic dipole moment which favours the electron injection of the dye into the conduction band of TiO_2. Finally, the introduction of alkylated aromatic units[17–19] at the two side *meso*-positions has led to a further improvement of performance, due to the minimisation of charge recombination arising from the dye aggregation.[20,21] Thanks to these developments, the PCE of porphyrin-sensitised devices has grown rapidly and has provided the new record PCE of 13%.[22] Nevertheless, despite the high efficiencies reported for some porphyrin dyes, the synthesis of unsymmetrical derivatives is problematic and generally results in low yielding multi-step procedures leading to the formation of several side-products.[23,24]

In this article, we report the synthesis of two porphyrin-based dyes (Fig. 1) and their employment as sensitisers in DSSCs. Both the molecules incorporate three triphenylamine (TPA) moieties as donor units and differ for the presence of either a thiophene or a furan ring in the π-bridge (A_3B-type).[12] The three bulky TPA units have been incorporated into the dyes in view of their combined electron-donating character and ability to negate dye aggregation on the TiO_2 surface.[12] Thiophene and furan residues have been incorporated into the π-bridge, allowing the role these heterocycles have in controlling device performance of this class of dyes. Thiophene and its derivatives have been extensively studied as π-spacers in sensitisers for DSSCs, due to their smaller resonance energy (29 kcal mol^{-1} for thiophene, 36 kcal mol^{-1} for benzene) which enhances the conjugation by lowering the energy required for charge transfer (CT).[25,26] The employment of furan as π-spacer should further improve the dye performance, due to its lower aromatic energy (16 kcal mol^{-1}). It has also been verified that furan shows comparable optical properties and charge carrier mobility with thiophene[27] and better solubility when incorporated in polyconjugated systems.[28] Moreover, the higher oxidation potential of furan should improve the hole location, hence the stability of the dye,[29] and its PCE when compared to its thiophene analogue.[27,30,31] However, previous work has shown that thiophene, rather than furan, when incorporated as π-bridges of porphyrin dyes results in better PCEs, presumably due to the more electron withdrawing character and/or improved interactions between the dye and TiO_2 due to thiophene moiety.[32–35]

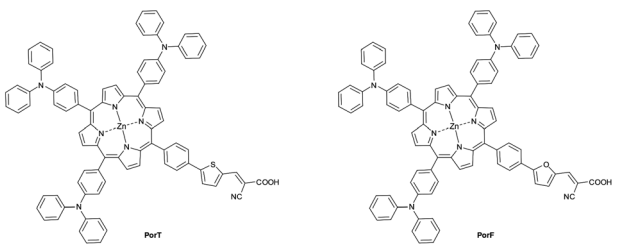

Fig. 1 Chemical structure of dyes **PorT** and **PorF**.

Results and discussion

Synthesis

Porphyrin based dyes **PorT** and **PorF** were synthesized according to Scheme 1. The synthesis of the central *meso*-substituted porphyrins was performed according to Lindsey's method[36,37]

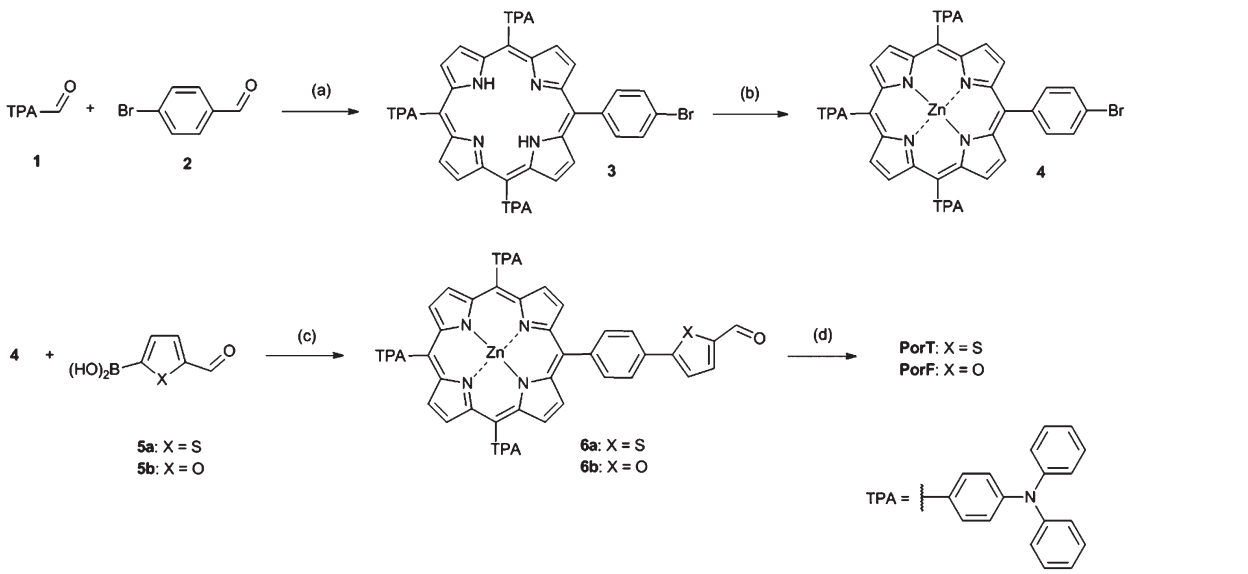

Scheme 1 Synthesis of dyes **PorT** and **PorF**. Conditions: (a) Pyrrole, DDQ, $BF_3{\cdot}O(C_2H_5)_2$, Et_3N, DCM, r.t., 3 h; (b) $Zn(OAc)_2$, MeOH, DCM, r.t., 18 h; (c) $Pd(dppf)Cl_2$, K_2CO_3 (2 M), DME, 80 °C, 2 d; (d) cyanoacetic acid, $Zn(OAc)_2$, THF, AcOH, 70 °C, 4 h.

(Scheme 1). 4-(Diphenylamino) benzaldehyde **1** and 4-bromobenzaldehyde **2** in 3.5/1 molar ratio were reacted with an excess of pyrrole to afford compound **3** in modest yield. This was then quantitatively converted to the Zn-based porphyrin **4**, by reaction with zinc acetate. A Suzuki cross-coupling reaction between **4** and the boronic acids **5a** and **5b**, was carried out affording aldehydes **6a** and **6b**, respectively. These were then reacted with cyanoacetic acid through a Knoevenagel condensation to obtain the final dyes **PorT** and **PorF**.

Optical and electrochemical properties

The UV-Vis absorption spectra of the two dyes recorded in solution (Fig. 2) show the typical behaviour of metalloporphyrins, consisting of an intense and sharp B-band and two weaker Q-bands.[38] The former, at 438 nm for **PorT** and 426 nm for **PorF**, have an intensity of the order of 10^5 M^{-1} cm^{-1}, whilst the latter, at 565 nm and 609 nm for **PorT** and 553 nm and 597 nm for **PorF**, are one order of magnitude weaker. The absorption maxima of **PorT** and **PorF** are at 650 nm and 625 nm, respectively, corresponding to optical bandgaps ($E_{G,OPT}$) of 1.91 eV and 1.98 eV.

The solution-based electrochemical properties of both dyes were explored by cyclic voltammetry (CV, Fig. 3) and square wave voltammetry (SWV, ESI Fig. S1†). Both dyes undergo pseudo-reversible one-electron reduction and oxidation. SWV allowed us to estimate the ionization potential (I_P), electron affinity (E_A) and fundamental band gap ($E_{G,F}$), respectively (Table 1). Both E_{red} and E_{ox} of **PorF** are more positive than those of **PorT**, of about 100 mV (−1.72 and 0.31 V for **PorT** and −1.62 and 0.40 V for **PorF**), resulting in more negative energy values for I_P and E_A.

Theoretical calculations

To gain insight in electronic properties of the two dyes, density functional theory (DFT) calculations were performed using Gaussian 09.[39] The optimized geometry shows a similar conformation for both the molecules, with the dihedral angles between the porphyrin and the appended benzene moieties of about 60°. Although this limits the conjugation throughout the molecule, a twisted structure could effectively decrease the dye aggregation by obstructing the formation of π-stacks among the porphyrin units.[40] Corresponding molecular orbitals for **PorT** and **PorF** are shown in Fig. 4. The HOMO is delocalised throughout the TPA donors and the porphyrin ring, while the LUMO is spread over the acceptor arm. This good separation is normally not found in porphyrin dyes having the π-bridge co-planar with the porphyrin core,[41,42]

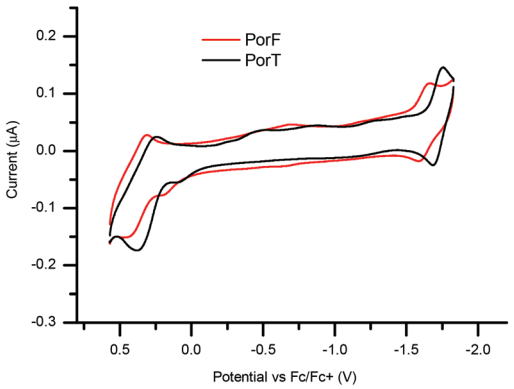

Fig. 3 Cyclic voltammetry plots of dyes **PorT** and **PorF** in DMF ($C = 10^{-3}$ M).

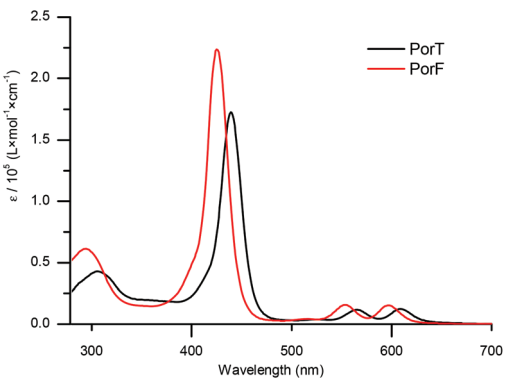

Fig. 2 UV-vis absorption spectra of dyes **PorT** and **PorF** in DMF ($C = 10^{-5}$ M).

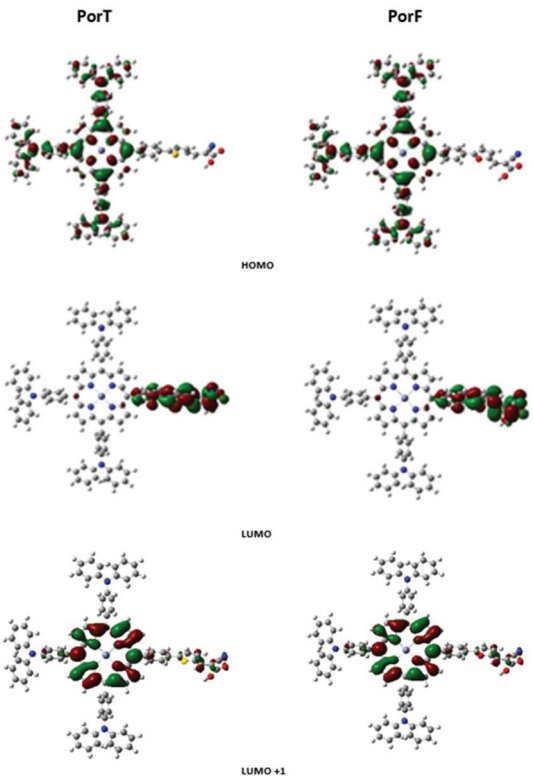

Fig. 4 Frontier molecular orbital representation of **PorT** and **PorF** calculated by DFT.

indicating that the absence of the intramolecular CT band is likely due to the twisted geometry of the molecule. Fig. 4 also shows that the spatial distribution of the LUMO+1 is confined on the porphyrin core, suggesting that an optical transition between the HOMO and the LUMO+1 would be more favourable. The estimated energy of the transition is 2.54 eV and 2.64 eV, for **PorT** and **PorF**, respectively, corresponding to a wavelength of 488 nm and 469 nm. The values are in good approximation with the experimental offset of the Soret bands ($S_0 \rightarrow S_2$) of both the dyes. This suggests that the π-bridge does not have a significant role in the light absorption, which presumably occurs due to the presence of the porphyrin core. However, the π-bridge should play a significant role in the extraction of electrons upon dye excitation.

A summary of the properties of the two dyes is provided in Table 1. It is worth observing that the calculated properties are in good agreement with both the experimentally estimated ones and those calculated in previous work for similar molecules.[43]

Table 1 Summary of dyes **PorT** and **PorF** physical parameters

Dye	$E_{G,OPT}$ [a]/eV	I_P [b]/eV (HOMO[c]/eV)	E_A [b]/eV (LUMO[c]/eV)	$E_{G,F}$ [d]/eV
PorT	1.9	−5.1 (−5.13)	−3.1 (−3.07)	2.0
PorF	2.0	−5.2 (−5.14)	−3.2 (−3.02)	2.0

[a] Calculated using the equation: $E_{G,OPT} = 1240/\lambda_{onset}$. [b] Estimated using the equations: I_P (eV) = −4.8 − E_{ox} and E_A (eV) = −4.8 − E_{red}.[44] [c] Values obtained by DFT calculation. [d] Calculated using the formula: $E_{G,F} = E_A - I_P$.

Device performance

The above dyes were tested as sensitisers in DSSCs by applying cobalt and iodide/triiodide redox electrolytes on 4 μm + 4 μm double layer TiO_2 films. The photovoltaic characteristics of these devices, A–D, measured at AM 1.5G irradiance (100 mW cm^{-2}), are tabulated in Table 2. For dye **PorF**, Device A, the highest PCE obtained is 4.1% with a V_{OC} of 0.700 V, a J_{SC} of 7.7 mA cm^{-2} and a FF of 75%. In turn, device B exhibits V_{OC} of 0.660 V, J_{SC} of 8.9 mA cm^{-2}, and PCE of 4.5%. Furthermore, employing the same cobalt and iodide/triiodide based redox electrolytes with **PorT** dye, labelled as devices C and D, respectively, the photovoltaic characteristics are tabulated in Table 2.

Table 2 Photovoltaic parameters of devices **A–D** measured under standard AM 1.5G illuminations at 100 mW cm^{-2}

Device	Dye	Electrolyte	J_{SC} [mA cm^{-2}]	V_{OC} [mV]	FF (%)	PCE [%]
A	**PorF**	Co^{2+}/Co^{3+}	7.7	700	0.75	4.1
B	**PorF**	I^-/I^{3-}	8.9	660	0.71	4.5
C	**PorT**	Co^{2+}/Co^{3+}	5.9	688	0.77	3.1
D	**PorT**	I^-/I^{3-}	8.1	606	0.74	3.6
Ref	**Y123**	I^-/I^3	12.7	749	0.76	7.3
Ref	**Y123**	Co^{2+}/Co^{3+}	12.7	808	0.78	8.0

The data show that having thiophene (**PorT**) closer to the surface of TiO_2 enhances the recombination compared to furan (**PorF**) dye, which is reflected in the lower V_{OC} of **PorT** dye with both electrolytes. To the best of our knowledge, these results are in contrast with related studies on porphyrin-based dyes. However, these results are in good agreement with several studies on metal-free push–pull dyes[27,31,45] which showed an increase in V_{OC} when the device is sensitised with a furan-based dye compared to its thiophene analogue. As suggested by the authors, this difference may be due to the enhanced suppression of the electron recombination between TiO_2 and electrolyte.

The incident photon-to-current conversion efficiency (IPCE) spectrum of the devices is shown in Fig. 5a (inset). The IPCE spectra of both the devices A and B have peak maxima at 450 and 620 nm and the tail goes up to 700 nm. The IPCE spectrum reflects closely the absorption spectra of dyes. The integrated current of IPCE spectra of devices is close to the measured current. The difference in the HOMO level of these dyes with the cobalt electrolyte redox energy level is large enough to provide a driving force for the dye regeneration. Transient photovoltage characterisation under open circuit voltage was performed to understand the differences in the photovoltaic parameters of devices with two different electrolytes. The plot of charge *vs.* potential for the devices A and B shows similar behaviour but at the same charge density the V_{OC} is higher for cobalt-based electrolyte (Fig. 5b) which is consistent with the difference in the energy level of these two electrolytes.

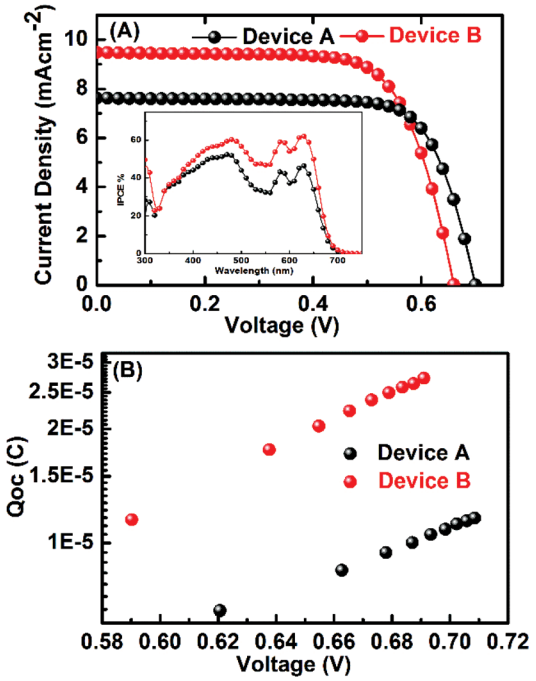

Fig. 5 (a) Photocurrent density *vs.* voltage (*J*–*V*) curves of devices A and B with **PorT** under standard AM 1.5G illumination. The inset is the IPCE of devices. (b) Charge *vs.* V_{OC} curves.

Conclusions

In conclusion, two porphyrin dyes containing furan and thiophene as π-conjugated spacers have been synthesized. The systematic modification of the dyes has allowed us to investigate the role this has on the optical and redox properties of the dyes together with its influence on DSSC device performance. Modification of this type leads to a significant change in the dyes solution optical and redox properties, with **PorT** having a lower estimated optical band gap. **PorF** gave rise to the best performing DSSC devices in terms of power conversion efficiencies, which was independent of the electrolyte used. This work is in contrast with related studies that have indicated that thiophene-based bridges tend to give rise to superior power conversion efficiencies, and indicates that the role the structure of the π-conjugated spacer has in determining device characteristics of porphyrin based dyes is dependent upon the parent structure of the porphyrin.

Experimental

General information

Chemicals were purchased from Sigma-Aldrich, TCI and Alfa Aesar, and were used without further purification. All reactions were run under an argon atmosphere. Solvents were purified using a PureSolv solvent purifier system. NMR spectra were performed with either a Bruker AVIII 400 MHz or a Bruker AVIII 500 MHz spectrometer and all reported chemical shifts are relative to TMS. Mass spectra were performed by the National Mass Spectroscopy Facility (NMSF), Swansea University (UK). UV-vis spectra were recorded on a PerkinElmer Lambda 25 instrument. Optically determined band gaps (E_{OPT}) were estimated using the absorption edge of the longest wavelength absorption (λ) using $E_{G,OPT}$ (eV) = (1240/λ(nm)). Cyclic voltammetry measurements were undertaken using a CH Instruments 440A electrochemical analyser using a platinum working electrode, a platinum wire counter electrode and a silver wire pseudo-reference electrode. Ferrocene was used as an external standard and all redox couples are reported *versus* the ferrocene/ferrocenium (Fc/Fc^+) redox couple, adjusted to 0.0 V. The solutions were prepared using dry DMF containing electrochemical grade tetrabutylammonium hexafluorophosphate (0.1 M) as the supporting electrolyte. The solutions were purged with nitrogen gas for 3 min prior to recording the electrochemical data.

Theoretical calculations

Density functional theory (DFT) calculations were performed using Gaussian 09, revision D.01.[39] Global minimum states were confirmed by absence from imaginary frequencies under ground-state geometry optimization followed by vibrational frequency calculations. All calculations were conducted with Becke's three-parameter hybrid and Lee–Yang–Parr's gradient corrected correlation (B3LYP) functional, 6-311G(d,p) basis set for H, C, N, O, S and Lanl2DZ for Zn, under vacuum.

Device fabrication and testing

State-of-the-art double layer mesoporous TiO_2 layer (4 μm thickness of 20 nm particle (DSL 18NR-T, DYESOL) plus 4 μm thickness of 400 nm light scattering particles (HPW-400NRD, CCIC)) were deposited on FTO conducting glass (Solar-4 mm, Nippon Sheet Glass Co, Ltd). The double layer TiO_2 film was sensitized by immersing it into a solution of the **PorF** and **PorT** dyes (0.025 mM) and chenodeoxycholic acid (1.25 mM) in a *tert*-butanol/acetonitrile mixture (1 : 1 v/v) for 13 h at room temperature. A platinized FTO conducting glass (LOF TECH 7, Pilkington) was used as a counter electrode. The composition of the iodide based electrolyte (Z960) is 1.0 M 1,3-dimethylimidazolium iodide, 0.5 M *tert*-butylpyridine, 0.03 M iodine, 0.05 M LiI, 0.1 M GuNCS in acetonitrile : valeronitrile (85 : 15 v/v) and the composition of the cobalt electrolyte is 0.22 M $[Co(bpy)_3](TFSI)_2$, 0.05 M $[Co(bpy)_3](TFSI)_3$, 0.1 M $LiClO_4$, and 0.2 M *tert*-butylpyridine in acetonitrile. Devices A and B were fabricated by using **PorF** with cobalt electrolyte and iodide/triiodide redox electrolyte, respectively. Devices C and D were fabricated by using **PorT** with cobalt electrolyte and iodide/triiodide redox electrolyte, respectively. An antireflection film (ARCTOP, Mihama Co.,) was attached on the photoanode side.

For photovoltaic measurements of the DSSCs, a solar simulator equipped with a 450 W xenon light source (Osram XBO 450) with a filter (Schott 113) was employed, whose power was regulated to the AM 1.5 solar standard by using a reference Si photodiode equipped with a colour-matched filter (KG-3, Schott) to reduce the mismatch in the region of 350–750 nm between the simulated light and AM 1.5 to less than 4%. The measurement-settling time between applying a voltage and measuring a current density for the *J–V* characterization of DSSCs was fixed to 80 ms with a Keithley model 2400 digital source meter. The photocurrent action spectra were measured with an Incident Photon-to-Current Conversion Efficiency (IPCE) test system. The modulation frequency used was about 2 Hz and light from a 300 W xenon lamp (ILC Technology, USA) was focused through a computer controlled Gemini-180 double monochromator (John Yvon Ltd, UK). A white light bias was used to bring the total light intensity on the device under testing closer to operating conditions. A light mask was used on the DSSCs, so the illuminated active area of DSCs was fixed to 0.159 cm^2.

Synthesis

5-(4-Bromophenyl)-10,15,20-tris(*N*,*N*-diphenylaniline)porphyrin 3. Pyrrole (0.750 mL, 10.8 mmol) and 4-bromobenzaldehyde **2** (0.500 g, 2.70 mmol) were added to a solution of 4-(diphenylamino)benzaldehyde **1** (2.50 g, 9.15 mmol) in degassed DCM (150 mL). $BF_3{\cdot}OEt_2$ (0.300 mL, 2.43 mmol) was added, and the mixture was stirred at r.t. for 4 h. Afterwards, DDQ (1.75 g, 7.71 mmol) was added and the resulting mixture was stirred for further 1 h. Et_3N (5 mL, 36.07 mmol) was then added and the mixture was stirred for further 30 min, filtered through a pad of silica and concentrated under reduced pressure. The crude compound was purified by column chrom-

atography (SiO_2, PE : DCM, 3 : 2), affording **3** (0.483 g, 15%) as a dark green powder. m.p. 212–214 °C; δ_H (500 MHz, $CDCl_3$, TMS) 9.01 (m, 6H), 8.83 (d, *J* 4.7, 2H), 8.13–8.04 (m, 8H), 7.91 (d, *J* 8.3, 2H), 7.50–7.44 (m, 6H), 7.44–7.37 (m, 24H), 7.19–7.11 (m, 6H), −2.71 (s, 2H); δ_C (125 MHz, $CDCl_3$, TMS) 148.0, 147.8, 141.5, 136.2, 136.1, 135.9, 135.8, 135.8, 130.07, 129.7, 125.1, 125.1, 125.1, 125.0, 123.5, 123.5, 122.6, 121.5, 121.5, 120.7, 120.4, 118.3; HRMS (NSI) *m*/*z* calcd for $C_{80}H_{57}BrN_7$ $[M + 2H]^{2+}$: 597.6963; found 597.6956.

5-(4-Bromophenyl)-10,15,20-tris(*N*,*N*-diphenylaniline) porphyrinato zinc(II) 4. A mixture of $Zn(OAc)_2$ (0.250 g, 1.36 mmol) in MeOH (50 mL) was added to a solution of **3** (0.140 g, 0.117 mmol) in DCM (150 mL). The resulting mixture was stirred overnight at r.t. and then poured into water (150 mL). The organic fraction was washed with brine (150 mL) and water (150 mL) consecutively, dried over $MgSO_4$, filtered and then concentrated under reduced pressure. The crude product was purified by column chromatography (SiO_2, DCM), affording **4** (0.141 g, 96%) as a dark purple solid. m.p. 262–265 °C; δ_H (400 MHz, $CDCl_3$, TMS) 9.15–9.09 (m, 6H), 8.94 (d, *J* 4.7, 2H), 8.09 (m, 8H), 7.90 (d, *J* 8.4, 2H), 7.51–7.44 (m, 6H), 7.43 (m, 24H), 7.19–7.11 (m, 6H); δ_C (100 MHz, $CDCl_3$, TMS) 150.7, 150.6, 150.5, 149.9, 148.1, 148.1, 147.5, 142.1, 136.8, 136.7, 136.0, 135.6, 135.6, 132.4, 132.3, 132.2, 131.7, 129.9, 129.6, 125.1, 124.9, 123.4, 122.3, 121.6, 121.4, 121.3, 119.3; HRMS (NSI) *m*/*z* calcd for $C_{80}H_{55}N_7BrZn$ $[M + H]^+$: 1256.2988; found 1256.3001.

5-(4-(5′-Formyl)thienyl)phenyl-10,15,20-tris(*N*,*N*-diphenylaniline) porphyrinato zinc(II) 6a. An aqueous solution of 2 M K_2CO_3 (0.200 mL, 0.400 mmol) was added to a mixture of **4** (0.100 g, 79.4 μmol) and 5-formyl-2-thiopheneboronic acid **5a** (18.6 mg, 0.119 mmol) in DME (10 mL) and the resulting mixture was degassed with N_2 for 30 min. $Pd(dppf)Cl_2$ (6.2 mg, 3.97 μmol) was added and the solution was stirred at 80 °C for 48 h. The mixture was then allowed to cool to r.t., poured into water (30 mL) and extracted with DCM (3 × 30 mL). The combined organic extracts were dried over $MgSO_4$, filtered and then concentrated under reduced pressure. The crude compound was purified by column chromatography (SiO_2, DCM), affording **6a** (77.8 mg, 76%) as a purple solid. m.p. 222–224 °C; δ_H (400 MHz, $CDCl_3$, TMS) 10.00 (s, 1H), 9.16–9.09 (m, 6H), 9.00 (d, *J* 4.7, 2H), 8.31 (d, *J* 8.3, 2H), 8.12–8.05 (m, 8H), 7.90 (d, *J* 3.9, 1H), 7.72 (d, *J* 3.9, 1H), 7.47 (m, 6H), 7.44–7.39 (m, 24H), 7.18–7.11 (m, 6H); δ_C (100 MHz, $CDCl_3$, TMS) 183.1, 154.4, 150.8, 150.6, 150.6, 149.9, 148.1, 148.1, 147.6, 144.5, 142.9, 137.8, 136.8, 136.7, 135.6, 135.5, 135.46, 132.4, 132.4, 132.4, 132.3, 132.2, 131.6, 129.6, 125.0, 125.0, 124.8, 124.7, 123.4, 121.6, 121.5, 121.4, 121.3, 119.6; HRMS (NSI) *m*/*z* calcd for $C_{85}H_{58}N_7OSZn$ $[M + H]^+$: 1288.3710; found 1288.3707.

5-(4-(5′-Formyl)furan)phenyl-10,15,20-tris(*N*,*N*-diphenylaniline) porphyrinato zinc(II) 6b. An aqueous solution of 2 M K_2CO_3 (0.200 mL, 0.400 mmol) was added to a mixture of **4** (0.100 g, 79.4 μmol) and 5-formyl-2-furanboronic acid **5b** (16.6 mg, 0.119 mmol) in DME (10 mL) and the resulting mixture was degassed with N_2 for 30 min. $Pd(dppf)Cl_2$ (6.2 mg, 3.97 μmol) was added and the solution was stirred at 80 °C for 48 h. The mixture was then allowed to cool to r.t., poured into water (30 mL) and extracted with DCM (3 × 30 mL). The combined organic extracts were dried over $MgSO_4$, filtered and then concentrated under reduced pressure. The crude compound was purified by column chromatography (SiO_2, PE : DCM, 1 : 4), affording **6b** (75.8 mg, 75%) as a purple solid. m.p. 230–233 °C; δ_H (400 MHz, $CDCl_3$, TMS) 9.76 (s, 1H), 9.13 (m, 6H), 8.98 (d, *J* 4.7, 2H), 8.33 (d, *J* 8.4, 2H), 8.23 (d, *J* 8.3, 2H), 8.13–8.06 (m, 6H), 7.47 (m, 7H), 7.42 (m, 24H), 7.18–7.10 (m, 7H); δ_C (100 MHz, $CDCl_3$, TMS) 177.5, 159.8, 152.6, 150.8, 150.6, 150.6, 149.9, 148.1, 148.1, 147.6, 144.8, 136.8, 136.7, 135.6, 135.6, 135.3, 132.5, 132.4, 132.3, 132.3, 131.7, 129.7, 128.3, 125.0, 125.0, 123.8, 123.4, 121.6, 121.5, 121.5, 121.4, 119.8, 108.4; HRMS (MALDI) *m*/*z* calcd for $C_{85}H_{57}N_7O_2Zn$ $[M]^{+\bullet}$: 1271.3865; found 1271.3872.

2-Cyano-3-(5-(4-(10,15,20-tris(*N*,*N*-diphenylaniline))porphyrinato zinc(II)-yl)phenyl)thienyl acrylic acid (PorT). Compound **6a** (0.100 g, 77.5 μmol) and cyanoacetic acid (29.7 mg, 0.349 mmol) were dissolved in a mixture of THF and acetic acid (12 mL, 1 : 1, v : v). Ammonium acetate (29.9 mg, 0.388 mmol) and zinc acetate dihydrate (68.0 mg, 0.310 mmol) were added and the resulting mixture was stirred for 4 h at 70 °C under N_2. The mixture was allowed to cool to r.t. and water (50 mL) was added. After stirring for further 10 min at r.t., the precipitate was filtered off, washed with water (50 mL) and dried under vacuum. The crude compound was purified by column chromatography (SiO_2, DCM : MeOH, 9 : 1) affording **PorT** (0.100 g, 95%) as a dark green solid. m.p. 264–267 °C; δ_H (400 MHz, d_6-DMSO, TMS, 80 °C) 8.96–8.90 (m, 6H), 8.31–8.25 (m, 3H), 8.19–8.15 (m, 2H), 8.12–8.04 (m, 6H), 7.50–7.43 (m, 12H), 7.41–7.34 (m, 18H), 7.21–7.14 (m, 6H); HRMS (NSI) *m*/*z* calcd for $C_{88}H_{59}N_8O_2SZn$ $[M + H]^+$: 1355.3768; found 1355.3770.

2-Cyano-3-(5-(4-(10,15,20-tris(*N*,*N*-diphenylaniline))porphyrinato zinc(II)-yl)phenyl)furyl acrylic acid (PorF). Compound **6b** (0.100 g, 78.5 μmol) and cyanoacetic acid (30.0 mg, 0.353 mmol) were dissolved in a mixture of THF and acetic acid (12 mL, 1 : 1, v : v). Ammonium acetate (30.3 mg, 0.392 mmol) and zinc acetate dihydrate (68.9 mg, 0.314 mmol) were added and the resulting mixture was stirred for 4 h at 70 °C under N_2. The mixture was allowed to cool to r.t. and water (50 mL) was added. After stirring for further 10 min at r.t., the precipitate was filtered off, washed with water (50 mL) and dried under vacuum. The crude compound was purified by column chromatography (SiO_2, DCM : MeOH, 9 : 1) affording **PorF** (97.9 mg, 93%) as a dark green solid. m.p. 230–233 °C; δ_H (400 MHz, d_6-DMSO, TMS) 8.97–8.93 (m, 6H), 8.87 (d, *J* 4.6, 2H), 8.30 (s, 4H), 8.11–8.06 (m, 6H), 7.90 (s, 1H), 7.55 (d, *J* 3.6, 1H), 7.50–7.45 (m, 12H), 7.40–7.35 (m, 18H), 7.20–7.15 (m, 6H); HRMS (NSI) *m*/*z* calcd for $C_{88}H_{59}N_8O_3Zn$ $[M - H]^-$: 1337.3851; found 1337.3866.

Conflicts of interest

There are no conflicts to declare.

Acknowledgements

GC and MC thank the EPSRC for funding (EP/E036244/1, EP/J500434/1). GC thanks the National Mass Spectroscopy Facility (NMSF), Swansea University (UK). S. M. A. acknowledges the Ministry of Higher Education and Scientific Research in Iraq and Kufa University for funding and support. We acknowledge Swiss National Science Foundation for financial support with the project entitled as "Fundamental studies of mesoscopic devices for solar energy conversion" with project number 20020_169695. P. Y. acknowledges the support from Swiss Government Excellence postdoctoral fellowship.

Notes and references

1 J. Gong, K. Sumathy, Q. Qiao and Z. Zhou, *Ren. Sust. Energ. Rev.*, 2017, **68**(1), 234–246.
2 B. O'Regan and M. Gratzel, *Nature*, 1991, **353**, 737–740.
3 M. Liang and J. Chen, *Chem. Soc. Rev.*, 2013, **42**, 3453–3488.
4 M. G. Walter, A. B. Rudine and C. C. Wamser, *J. Porphyrins Phthalocyanines*, 2010, **14**, 759–792.
5 A. Harriman, *J. Chem. Soc., Faraday Trans. 2*, 1981, **77**, 1281–1291.
6 P. K. Goldberg, T. J. Pundsack and K. E. Splan, *J. Phys. Chem. A*, 2011, **115**, 10452–10460.
7 J. Feng, Y. Jiao, W. Ma, M. K. Nazeeruddin, M. Grätzel and S. Meng, *J. Phys. Chem. C*, 2013, **117**, 3772–3778.
8 A. Mishra, M. K. R. Fischer and P. Bäuerle, *Angew. Chem., Int. Ed.*, 2009, **48**, 2474–2499.
9 F. Arkan and M. Izadyar, *Mater. Chem. Phys.*, 2017, **196**, 142–152.
10 T. D. Santos, A. Morandeira, S. Koops, A. J. Mozer, G. Tsekouras, Y. Dong, P. Wagner, G. Wallace, J. C. Earles, K. C. Gordon, D. Officer and J. R. Durrant, *J. Phys. Chem. C*, 2010, **114**, 3276–3279.
11 A. Kay and M. Graetzel, *J. Phys. Chem.*, 1993, **97**, 6272–6277.
12 M. Urbani, M. Grätzel, M. K. Nazeeruddin and T. Torres, *Chem. Rev.*, 2014, **114**, 12330–12396.
13 M. K. Nazeeruddin, R. Humphry-Baker, D. L. Officer, W. M. Campbell, A. K. Burrell and M. Grätzel, *Langmuir*, 2004, **20**, 6514–6517.
14 S. Cherian and C. C. Wamser, *J. Phys. Chem. B*, 2000, **104**, 3624–3629.
15 M. S. Kang, S. H. Kang, S. G. Kim, I. T. Choi, J. H. Ryu, M. J. Ju, D. Cho, J. Y. Lee and H. K. Kim, *Chem. Commun.*, 2012, **48**, 9349–9351.
16 R. B. Ambre, G.-F. Chang, M. R. Zanwar, C.-F. Yao, E. W.-G. Diau and C.-H. Hung, *Chem. – Asian J.*, 2013, **8**, 2144–2153.
17 T. Higashino, K. Kawamoto, K. Sugiura, Y. Fujimori, Y. Tsuji, K. Kurotobi, S. Ito and H. Imahori, *ACS Appl. Mater. Interfaces*, 2016, **8**, 15379–15390.
18 A. Yella, H.-W. Lee, H. N. Tsao, C. Yi, A. K. Chandiran, M. K. Nazeeruddin, E. W.-G. Diau, C.-Y. Yeh, S. M. Zakeeruddin and M. Grätzel, *Science*, 2011, **334**, 629–634.
19 C.-L. Wang, J.-Y. Hu, C.-H. Wu, H.-H. Kuo, Y.-C. Chang, Z.-J. Lan, H.-P. Wu, E. Wei-Guang Diau and C.-Y. Lin, *Energy Environ. Sci.*, 2014, **7**, 1392–1396.
20 V. Villari, P. Mineo, E. Scamporrino and N. Micali, *RSC Adv.*, 2012, **2**, 12989–12998.
21 N. C. Maiti, S. Mazumdar and N. Periasamy, *J. Phys. Chem. B*, 1998, **102**, 1528–1538.
22 S. Mathew, A. Yella, P. Gao, R. Humphry-Baker, B. F. E. Curchod, N. Ashari-Astani, I. Tavernelli, U. Rothlisberger, M. K. Nazeeruddin and M. Grätzel, *Nat. Chem.*, 2014, **6**, 242.
23 S. J. Lee, C. D. Malliakas, M. G. Kanatzidis, J. T. Hupp and S. T. Nguyen, *Adv. Mater.*, 2008, **20**, 3543–3549.
24 K. E. Splan and J. T. Hupp, *Langmuir*, 2004, **20**, 10560–10566.
25 S. Sharma, N. Zamoshchik and M. Bendikov, *Isr. J. Chem.*, 2014, **54**, 712–722.
26 J. H. Delcamp, Y. Shi, J.-H. Yum, T. Sajoto, E. Dell'Orto, S. Barlow, M. K. Nazeeruddin, S. R. Marder and M. Grätzel, *Chem. – Eur. J.*, 2013, **19**, 1819–1827.
27 S. Qu, B. Wang, F. Guo, J. Li, W. Wu, C. Kong, Y. Long and J. Hua, *Dyes Pigm.*, 2012, **92**, 1384–1393.
28 O. Gidron and M. Bendikov, *Angew. Chem., Int. Ed.*, 2014, **53**, 2546–2555.
29 P. Shen, X. Liu, S. Jiang, Y. Huang, L. Yi, B. Zhao and S. Tan, *Org. Electron.*, 2011, **12**, 1992–2002.
30 R. Li, X. Lv, D. Shi, D. Zhou, Y. Cheng, G. Zhang and P. Wang, *J. Phys. Chem. C*, 2009, **113**, 7469–7479.
31 J. Jia, Y. Zhang, P. Xue, P. Zhang, X. Zhao, B. Liu and R. Lu, *Dyes Pigm.*, 2013, **96**, 407–413.
32 H. Jia, X. Ju, M. Zhang, Z. Ju and H. Zheng, *Phys. Chem. Chem. Phys.*, 2015, **17**, 16334–16340.
33 N. V. Krishna, J. V. S. Krishna, S. P. Singh, L. Giribabu, L. Han, I. Bedja, R. K. Gupta and A. Islam, *J. Phys. Chem. C*, 2017, **121**, 6464–6477.
34 M. Sreenivasu, A. Suzuki, M. Adachi, C. V. Kumar, B. Srikanth, S. Rajendar, D. Rambabu, R. S. Kumar, P. Mallesham, N. V. B. Rao, M. S. Kumar and P. Y. Reddy, *Chem. – Eur. J.*, 2014, **20**, 14074–14083.
35 S. Eu, S. Hayashi, T. Umeyama, A. Oguro, M. Kawasaki, N. Kadota, Y. Matano and H. Imahori, *J. Phys. Chem. C*, 2007, **111**, 3528–3537.
36 J. S. Lindsey, H. C. Hsu and I. C. Schreiman, *Tetrahedron Lett.*, 1986, **27**, 4969–4970.
37 J. S. Lindsey, I. C. Schreiman, H. C. Hsu, P. C. Kearney and A. M. Marguerettaz, *J. Org. Chem.*, 1987, **52**, 827–836.
38 J. Karolczak, D. Kowalska, A. Lukaszewicz, A. Maciejewski and R. P. Steer, *J. Phys. Chem. A*, 2004, **108**, 4570–4575.
39 M. J. Frisch, G. W. Trucks, H. B. Schlegel, G. E. Scuseria, M. A. Robb, J. R. Cheeseman, G. Scalmani, V. Barone, B. Mennucci, G. A. Petersson, H. Nakatsuji, M. Caricato, X. Li, H. P. Hratchian, A. F. Izmaylov, J. Bloino, G. Zheng, J. L. Sonnenberg, M. Hada, M. Ehara, K. Toyota, R. Fukuda, J. Hasegawa, M. Ishida, T. Nakajima, Y. Honda, O. Kitao, H. Nakai, T. Vreven, J. A. Montgomery Jr., J. E. Peralta, F. Ogliaro, M. J. Bearpark, J. Heyd, E. N. Brothers,

K. N. Kudin, V. N. Staroverov, R. Kobayashi, J. Normand, K. Raghavachari, A. P. Rendell, J. C. Burant, S. S. Iyengar, J. Tomasi, M. Cossi, N. Rega, N. J. Millam, M. Klene, J. E. Knox, J. B. Cross, V. Bakken, C. Adamo, J. Jaramillo, R. Gomperts, R. E. Stratmann, O. Yazyev, A. J. Austin, R. Cammi, C. Pomelli, J. W. Ochterski, R. L. Martin, K. Morokuma, V. G. Zakrzewski, G. A. Voth, P. Salvador, J. J. Dannenberg, S. Dapprich, A. D. Daniels, Ö. Farkas, J. B. Foresman, J. V. Ortiz, J. Cioslowski and D. J. Fox, *Gaussian 09*, Gaussian, Inc., Wallingford, CT, USA, 2009.

40 I. Beletskaya, V. S. Tyurin, A. Y. Tsivadze, R. Guilard and C. Stern, *Chem. Rev.*, 2009, **109**, 1659–1713.

41 S. Arrechea, J. N. Clifford, L. Pellejà, A. Aljarilla, P. de la Cruz, E. Palomares and F. Langa, *Dyes Pigm.*, 2016, **126**, 147–153.

42 A. Aljarilla, J. N. Clifford, L. Pelleja, A. Moncho, S. Arrechea, P. d. l. Cruz, F. Langa and E. Palomares, *J. Mater. Chem. A*, 2013, **1**, 13640–13647.

43 S. Karthikeyan and J. Y. Lee, *J. Phys. Chem. A*, 2013, **117**, 10973–10979.

44 C. M. Cardona, W. Li, A. E. Kaifer, D. Stockdale and G. C. Bazan, *Adv. Mater.*, 2011, **23**, 2367–2371.

45 J. T. Lin, P.-C. Chen, Y.-S. Yen, Y.-C. Hsu, H.-H. Chou and M.-C. P. Yeh, *Org. Lett.*, 2009, **11**, 97–100.